Helical bunching and symmetry lowering inducing multiferroicity in Fe langasites

Laura Chaix, Rafik Ballou, Andres Cano, Sylvain Petit, Sophie de Brion, Jacques Ollivier, Louis-Pierre Regnault, Eric Ressouche, Evan Constable, Claire Colin, et al.

Helical bunching and symmetry lowering inducing multiferroicity in Fe langasites

L. Chaix,[1,2,3,4,*] R. Ballou,[2,3] A. Cano,[5] S. Petit,[6] S. de Brion,[2,3] J. Ollivier,[1] L.-P. Regnault,[7,3] E. Ressouche,[7,3] E. Constable,[2,3] C. V. Colin,[2,3] J. Balay,[2,3] P. Lejay,[2,3] and V. Simonet[2,3,†]

[1]*Institut Laue-Langevin, 6 rue Jules Horowitz, 38042 Grenoble, France*
[2]*Institut Néel, CNRS, 38042 Grenoble, France*
[3]*Université Grenoble Alpes, 38042 Grenoble, France*
[4]*Stanford Institute for Materials and Energy Sciences, SLAC National Accelerator Laboratory, Menlo Park, California 94025, USA*
[5]*CNRS, Univ. Bordeaux, ICMCB, UPR 9048, F-33600 Pessac, France*
[6]*CEA, Centre de Saclay, /DSM/IRAMIS/ Laboratoire Léon Brillouin, 91191 Gif-sur-Yvette,France*
[7]*SPSMS-MDN, INAC, 38054 Grenoble, France*

(Dated: June 20, 2015)

In the chiral $Ba_3(Nb,Ta)Fe_3Si_2O_{14}$ langasites, the triangle-based helical magnetic order is revisited. It follows from the observation by neutron scattering of additional magnetic satellites and gaps in the spin waves spectra. These so-far undetected features are explained by a bunching of the magnetic helices due to single-ion anisotropy, and by a departure of the in-plane magnetic moments from the 120° arrangement due to a structural loss of the 3-fold axis. These weak modulations of the crystallographic and magnetic structures are shown to be responsible for a spin-induced electric polarization in zero and finite magnetic field, thus ascertaining the multiferroicity of these attractive materials.

PACS numbers: 75.85.+t, 75.25.-j, 75.30.Ds, 75.30.Gw

The quest for novel magnetic orders triggering multiferroicity and strong magnetoelectric couplings attracts a great deal of research attention, justified both by opportunities for technological applications and fundamental issues [1–12]. In this context, iron-based langasites are very promising materials [13]. These systems display an unusual example of "multi-chiral" magnetic order in which a helical modulation superimposes on a 120°-spin structure [14–16]. This magnetic order is induced purely by symmetric exchange interactions and by the chirality of the crystal structure, rather than by antisymmetric Dzyaloshinskii-Moriya (DM) exchange couplings as in most non-centrosymmetric helical magnets. In addition, there is an increasing number of publications addressing the magnetoelectric and multiferroic potential of these compounds. The magnetoelectric effect has been demonstrated at both static [17] and dynamical levels [18]. In addition, Zhou *et al.* [19] have reported the emergence of an electric polarization associated to the magnetic order. The onset of ferroelectricity has subsequently been confirmed by Lee et al. [20], who also have demonstrated the manipulation of the polarization by the application of a magnetic field. At zero-field, however, the polar axes reported in both of these works are different, and the precise mechanism behind ferroelectricity in Fe langasites is still unknown.

Magnetically-induced ferroelectricity in many multiferroic cycloidal magnets, like $TbMnO_3$, is due to the so-called inverse DM mechanism [6–8]. However, this mechanism is ineffective for the reported helical structure of the langasites [21]. The possibilities of an electric polarization induced by a helical-type of magnetic order, and/or by a triangular-type of magnetic order, seem indeed to be less straightforward [22]. In $RbFe(MoO_4)_2$ for instance, which combines 120° magnetic moments and magnetic helices, similarly to the Fe langasite, it was first proposed that multiferroicity is promoted by the triangular chirality [23], then by the ferroaxial character of the lattice [24], before it was established to be a consequence of the DM interaction [25, 26]. On the other hand, in the context of Mott insulators, it has been shown theoretically that the electric polarization can be induced by distorted 120°-spin structures via high-order contributions to the exchange interactions (i.e. irrespective of spin-orbit coupling) [27].

In this article, we address this issue and show that a new mechanism of spin-induced ferroelectricity is realized in the Fe-based $Ba_3(Nb,Ta)Fe_3Si_2O_{14}$ langasites. Neutron scattering experiments reveal new features in the magnetic properties of these compounds, especially a bunching of the helicoidal state combined with a symmetry lowering. These features, intimately related to magnetic anisotropies, appeared to be crucial for the understanding of the multiferroic behavior and led us to propose a phenomenological model that explains the zero-field and the field-induced electric polarization.

$Ba_3NbFe_3Si_2O_{14}$ can be taken as the reference compound. This system crystallizes in the non-polar non-centrosymmetric space group P321, in which the magnetic Fe^{3+} $S = 5/2$ ions form a triangular lattice of triangles in the ab-plane (see Fig. 1). The magnetic order observed below $T_N = 27$ K has been rationalized accord-

*Corresponding author: lchaix@stanford.edu
†Corresponding author: virginie.simonet@neel.cnrs.fr

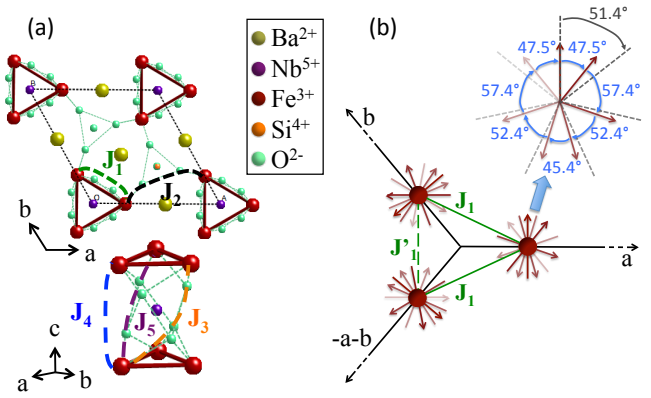

FIG. 1: (Color online) (a) $Ba_3NbFe_3Si_2O_{14}$ crystallographic structure in the *ab*-plane and along the *c*-axis, with five magnetic exchange paths J_1 to J_5. (b) Schematic representation of the revisited magnetic structure projected along the *c*-axis. The 3-fold axis is broken leading to different J_1 interactions (case of an isosceles triangle represented). The bunching of the helices is reported through the successive angles between consecutive magnetic moments along *c*, deviating from the regular angle $2\pi\tau$=51.4°.

ing to the spin Hamiltonian [14, 15, 28–30]:

$$\mathcal{H} = \sum_{(ij)} J_{ij}\mathbf{S}_i \cdot \mathbf{S}_j + \sum_{(ij)_\triangle} D(\mathbf{S}_i \times \mathbf{S}_j)_z. \qquad (1)$$

Here the first term describes the exchange interactions, where the sum runs over the spin pairs connected by the different paths shown in Fig. 1 (a). The nearest- and next-nearest-neighbor interactions J_1 and J_2 in the *ab*-plane are both AFM. This generates magnetic frustration within the Fe triangles and causes the 120° spin structure. Among the three AFM exchange couplings between adjacent *ab*-planes, the strongest one (J_3 or J_5) is determined by the structural chirality. These couplings generate the helical modulation of the 120° structure along the *c*-axis. The propagation vector $\vec{\tau} = (0, 0, 0.1429 \approx 1/7)$ of this modulation depends on the balance between the 3 inter-plane interactions J_3 to J_5. The second term in Eq. (1), where the sum runs over the spin pairs within the triangles, corresponds to the additional DM interactions. Considering a symmetry-allowed *D* vector along the *c* direction, its role restricts the spins to the *ab*-plane and imposes the triangular chirality [31].

We have revised this structure by carrying out single-crystal neutron scattering measurements on two members of the Fe langasite family with Nb or Ta on the 1*a* Wyckoff site. The two single-crystals, grown by floating zone method in an image furnace [17], display opposite structural chiralities. The experiments were done on two spectrometers installed at the Institut Laue Langevin: IN5 time-of-flight spectrometer using unpolarized neutrons, and CRG-CEA IN22 triple-axis spectrometer, equipped with CRYOPAD, using polarized neutrons and allowing longitudinal polarization analysis. Scattering intensities were collected on IN5 at 1.5 K, for both crystals in rotation about the *a* zone axis, with an incident wavelength of 4 Å. The inelastic spectra of the Nb compound were also measured on IN22 at 2 K with a final wavevector fixed to 2.66 $Å^{-1}$. The crystal was oriented with the *a* zone axis vertical so as to probe the (b^*, c^*) scattering plane. On IN22, two types of measurements were carried out using different monochromator-analyser configurations: Heusler-Heusler (H-H) and Graphite-Heusler (G-H). The former allows us to discriminate the magnetic and chiral contributions from the nuclear one, whereas the latter increases the incident neutron flux and allows us to determine the chiral scattering from an unpolarized beam [15], hence with a larger flux.

The intensity maps at zero energy measured on IN5 for the Nb and Ta compounds are shown in Figs. 2(a) and (b) respectively. The magnetic properties of the Ta compound are very close to the Nb one [17, 32]: same helical modulation of the 120° spin structure with T_N = 28 K, but with a slightly different propagation vector $\vec{\tau}$ =(0, 0, 0.1385) due to a different balance of the inter-plane exchange interactions. This leads to the observation of magnetic satellites at $Q = |\vec{H} \pm \vec{\tau}|$ in Figs. 2. In addition to the first-order satellites, we clearly observe higher-order satellites at $Q = |\vec{H} \pm 2\vec{\tau}|$ and $Q = |\vec{H} \pm 3\vec{\tau}|$ in both compounds. These extra satellites are not compatible with a perfect helix. Moreover, the perfect 120° spin arrangement within the Fe triangles should produce an extinction of the magnetic structure factor along the [0 0 ℓ]* line. However, first-order satellites (0, 0, $\ell \pm \tau$) are also observed with the same temperature dependence as the (0, 1, $\ell \pm \tau$) magnetic satellites [31]. Note that τ, 2τ and 3τ satellites in the first Brillouin zone were also observed by magnetic resonant X-ray diffraction [33].

Polarized neutrons measurements with longitudinal polarization analysis on the Nb compound allowed us to extract the nuclear (σ_N), the magnetic (σ_M) and the chiral (σ_{ch}) scatterings [31], hence to identify the nuclear and/or magnetic nature of these extra peaks. The (0, 0, $\ell \pm \tau$) satellites have mainly a magnetic origin [see Fig. 2(c)], which clearly demonstrates that the relative orientation of the magnetic moments on the triangles deviates from 120°. This result suggests that the J_1 interactions within each triangle are not equivalent, which in turn is only possible in the presence of a structural distortion implying a loss of the 3-fold axis and leading to a space group of lower symmetry than P321. Concerning the high-order satellites, the second-order ones have a prominent nuclear contribution. This is usually attributed to a structural deformation following the magnetic modulation due to magneto elastic effects. The third-order satellites have mainly a magnetic contribution [see Fig. 2(c)] indicating a deformation of the magnetic helices.

The modification of the perfect helical modulation inferred from the existence of satellites allows further to understand details of the spin-wave spectrum, as we shall see below. As we can see in Fig. 3, the spectra of the Nb

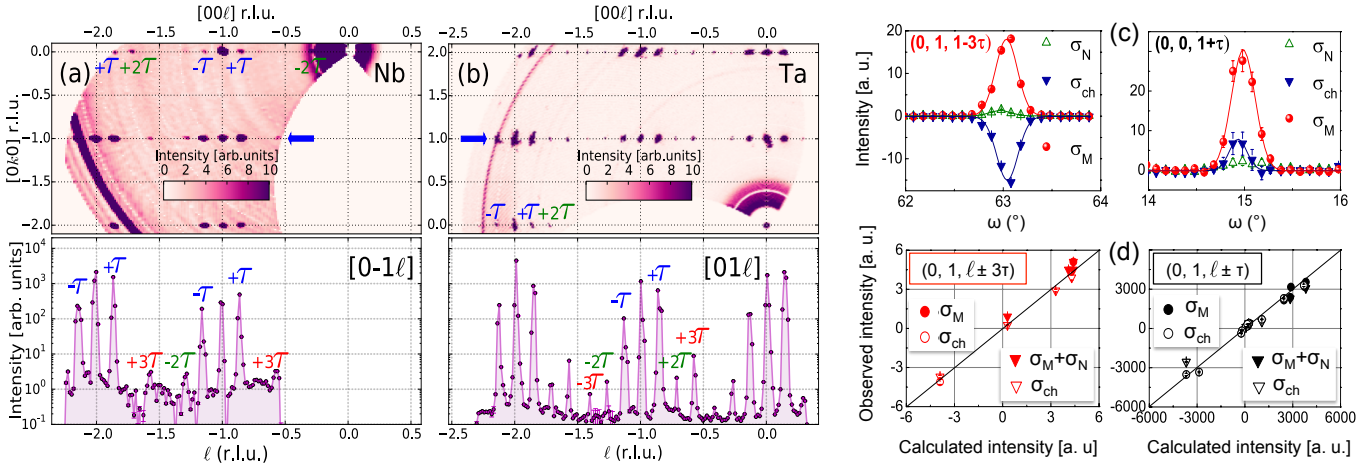

FIG. 2: (color online) Zero energy cut (integrated from -0.1 to 0.1 meV) from IN5 measurements at 1.5 K, on the Nb (a) and Ta (b) compounds. 1D cuts along the [0 1 ℓ]* directions are shown below the energy maps. The additional (0, 1, $\ell \pm 3\tau$), (0, 1, $\ell \pm 2\tau$) and (0, 0, $\ell \pm \tau$) satellites are shown in red, green and blue respectively. (c) corresponds to the magnetic (red), nuclear (green) and chiral (blue) contributions obtained from ω-scans at 2 K on IN22 with the H-H configuration. The magnetic and chiral contributions measured in the H-H (circles) and G-H (triangles) configurations for the main (0, 1, $\ell \pm \tau$) and extra (0, 1, $\ell \pm 3\tau$) satellites, versus the calculated contributions using the revised model, are displayed in (d).

and Ta compounds display two branches emerging from the magnetic satellites [28]. The high energy branch corresponds to spin components in the *ab*-plane while the low-energy branch is associated to spin components along the *c*-axis. The two branches are gapped, with a minimum of 0.2 meV (Ta) and 0.4 meV (Nb) for the *c*-branch whereas the *ab*-branch seems to present a much smaller gap (less than 0.1 meV) for both compounds (see Fig. 4 (b)) [15, 28]. In addition, a spectral weight extinction in the higher energy branch is clearly observed around 2.3 meV in both compounds (red arrows in Fig. 3). The main features of this spectrum were initially captured by the model of Eq. 1 within the linear-response approximation (see Fig. 3(c)) [28]. However, this model fails to reproduce the small gap and the extinction at ~ 2.3 meV in the *ab*-branch.

In order to reproduce these features, we have considered a generalization of the model of Eq. 1 introducing an extra single-ion anisotropy term with respect to the local 2-fold axes (a, b and $-a-b$ directions):

$$H_{sia} = K \sum_i S_{z,i}^2 \qquad (2)$$

with $K > 0$ for an easy-plane magnetization perpendicular to the local axis, and $K < 0$ for an easy-axis magnetization along the local axis. We first calculated the magnetic configuration stabilized by the new Hamiltonian including the single-ion anisotropy after a real-space mean-field energy minimization. We then calculated the corresponding magnetic and chiral elastic scatterings for the first and third order magnetic satellites, as well as the corresponding spin-wave spectrum. The additional single-ion anisotropy term allows us to quantitatively reproduce the magnetic and chiral neutron scattering of

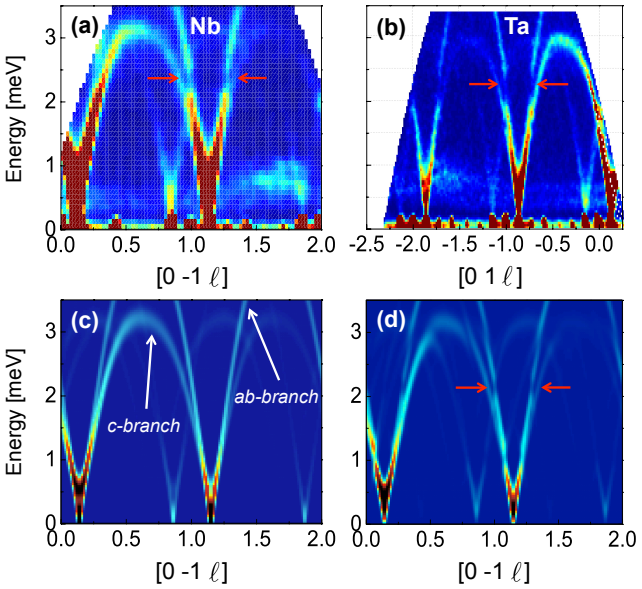

FIG. 3: (Color online) Spin-waves spectra of the Nb (a) and Ta (b) compounds measured along the [0 -1 ℓ]* and [0 1 ℓ]* directions respectively at 1.5 K on IN5. The red arrows show the spectral weight extinction. Corresponding spin waves calculations using the previous model of reference [28] (c) and using the model presently proposed (d) with the following parameters: $J_1 = 0.85$ meV, $J_2 = 0.24$ meV, $J_3 = 0.053$ meV, $J_4 = 0.017$ meV and $J_5 = 0.24$ meV, D= 0.02 meV, easy-plane anisotropy $K = 0.03$ meV.

the first-order (0, k, $\ell \pm \tau$) and extra (0, k, $\ell \pm 3\tau$) satellites (Figs. 2 (d)) and the weak features in the spin wave spectrum, namely the *ab*-branch gap and the extinction

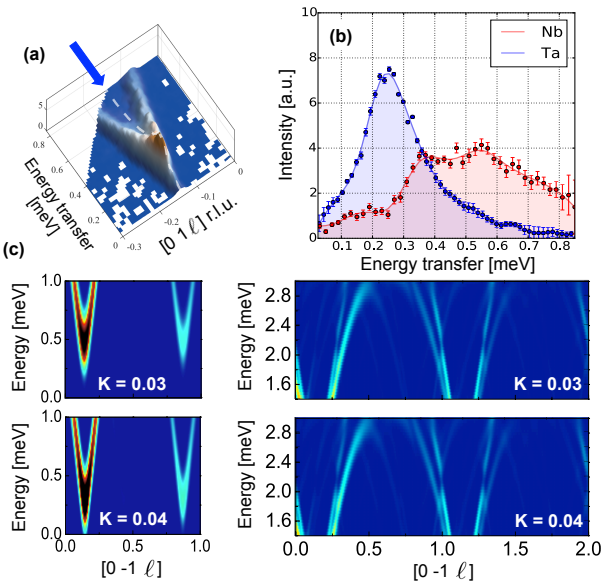

FIG. 4: (Color online) (a) Intensity map for the ([0 1 ℓ], E) plane in the Ta compound. The blue arrow shows the direction of the 1D-cut presented in (b): neutron scattering intensity versus the energy at the magnetic satellite position for the Ta and Nb-compounds. (c) Calculated evolution of the c-branch energy gap (left) and of the ab-branch extinction (right), w.r.t. the increase of the easy-plane anisotropy K.

at $\sim$ 2.3 meV (see Fig. 3 (d)). An easy-axis or an easy-plane anisotropy yield the same results, except that, for an easy-plane anisotropy, the DM interaction is still necessary to stabilize the in-plane magnetic order whereas it is optional for the easy-axis anisotropy. The best Hamiltonian parameters for an easy-plane anisotropy are given in the caption of figure 3 for the Nb compound. The final magnetic structure appears to be a bunched helix, as observed in some rare-earth intermetallics [34]. This means that the angles between adjacent magnetic moments along the helix axis deviate from the regular angle $2\pi\tau$=51.4°, being smaller close to the easy-axis/easy-plane of anisotropy and larger further away (see Fig. 1 (b)).

The two models with different magnetocrystalline anisotropy (easy-plane vs. easy-axis) can finally be discriminated by comparing Nb and Ta compounds. Indeed, the extinction at 2.3 meV in the spin-wave spectrum is more pronounced in the Ta compound (see Fig. 3) compared to the Nb one, whereas the gap of the c-component branch is, in contrast, smaller for the Ta (see Fig. 4). This points to two distinct sources of anisotropy : on the one hand, the easy-plane anisotropy, stronger for Ta (0.05 meV) than for Nb (0.03 meV) is responsible for the extinction in the ab-branch; on the other hand, the c-component of the DM vector essentially opens the gap in the c-branch; it then varies with the D/K ratio (see Fig. 4).

Our experimental observations thus reveal the following: (i) a deviation of the Fe intra-triangle spin order from a perfect 120° arrangement suggesting that the 3-fold axis of the P321 is likely lost in the Fe langasites, (ii) a bunched modulation of the magnetic helices along the c-axis, (iii) the microscopic contribution at the origin of this feature (additional easy-plane anisotropy). These results have important consequences in regards the multiferroic properties of these systems. The loss of the 3-fold axis was already suggested from Mössbauer spectroscopy [32] in a model-dependent analysis. This assumption of a structural distortion was also an ingredient of the phenomenological model proposed to explain the magnetoelectric atomic rotation mode probed by THz spectroscopy [18]. Last, it is consistent with the phonon spectrum [35], and with an electric polarization developing along the a-axis, as predicted from ab-initio calculations [36] and recently evidenced experimentally in zero-magnetic field [20].

In fact, the P321 space group allows the magnetoelectric coupling of the form:

$$F_{ME} = \alpha\{P_x(\mathbf{S}_1-\mathbf{S}_2)\cdot\mathbf{S}_3-\frac{1}{\sqrt{3}}P_y[(\mathbf{S}_1+\mathbf{S}_2)\cdot\mathbf{S}_3-2\mathbf{S}_1\cdot\mathbf{S}_2]\}$$

where y and x stand respectively for the [1 0 0] and [1 2 0] real space directions perpendicular to each other, and $\mathbf{S}_1$ to $\mathbf{S}_3$ are the three consecutive magnetic moments on a triangle (see Fig. 1). This coupling originates from the symmetric Heisenberg exchange, and its form is identical to the one discussed in [27]. The presence of such a coupling means that a spin-induced electric polarization has to be expected whenever the spin arrangement deviates from the perfect 120° structure. This polarization will lie in the ab-plane. Thus, the new magnetic structure deduced from our experiments is compatible with the results of Lee *et al.* [20] rather than those of Zhou *et al.* [19].

An enhanced polarization induced by a magnetic field has also been reported in [20]. This can also be understood on the basis of the above coupling, although it is even more subtly related to the revised magnetic structure. In this case, at each triangle, the 120° spin-structure is additionally deformed by the Zeeman coupling, which produces an extra local contribution to the electric polarization. In the perfect helical structure, these individual field-induced contributions coming from the different layers of the helix rotate along the c axis in such a way that they cancel each other. The bunching of the helical structure, however, modifies this rotation, and eventually enables an overall finite polarization induced by the magnetic field. We note that this happens even if the initial (zero-field) structure corresponds to a perfect 120° arrangement within the Fe triangles. We thus predict a stronger field-induced electric polarization in the Ta compound compared to the Nb one, since the single-ion anisotropy is larger and hence the bunching is more pronounced.

Our study has allowed us to lift the controversy about the multiferroic properties of the Fe langasite, by identifying weak modulations of the magnetic order with dras-

tic consequences. A departure from the 120° in-plane magnetic arrangement produces a spin-induced electric polarisation mostly along the a axis in zero magnetic field (for unbalanced 120 ° ferroelectric domain populations). A bunching of the helices is at the origin of a field-induced ferroelectricity. These two new mechanisms are triggered by symmetric exchange interactions and weak single-ion anisotropy, in contrast with the usually invoked DM interaction. Finally, the relation between the multiferroic properties and the overall chiral properties in this remarkable material is a promising issue that has still to be properly tackled.

Acknowledgments

We would like to acknowledge A. Hadj-Azzem and J. Debray for their help in the preparation of the samples, and V. Scagnoli for fruitful discussions.

[1] K. Aizu, Physical Review B **2**, 754 (1970).
[2] B. B. V. Aken, J.-P. Rivera, H. Schmid, and M. Fiebig, Nature **449**, 702 (2007).
[3] M. Fiebig, Journal of Physics D: Applied Physics **38**, R123 (2005).
[4] N. A. Hill, The Journal of Physical chemistry B **104**, 6694 (2000).
[5] W. Eerenstein, N. D. Mathur, and J. F. Scott, Nature **442**, 759 (2006).
[6] S.-W. Cheong and M. Mostovoy, Nature Matererials **6**, 13 (2007).
[7] I. A. Sergienko and E. Dagotto, Physical Review B **73**, 094434 (2006).
[8] H. Katsura, N. Nagaosa, and A. V. Balatsky, Physical Review Letters **95**, 057205 (2005).
[9] P. G. Radaelli, C. Vecchini, L. C. Chapon, P. J. Brown, S. Park, and S.-W. Cheong, Physical Review B **79**, 020404 (2009).
[10] R. D. Johnson, L. C. Chapon, D. D. Khalyavin, P. Manuel, P. G. Radaelli, and C. Martin, Physical Review Letters **108**, 067201 (2012).
[11] F. Yang, M. H. Tang, Z. Ye, Y. C. Zhou, X. J. Zheng, J. X. Tang, J. J. Zhang, and J. He, J. Appl. Phys. **102**, 044504 (2007).
[12] Y. Tokura, Science **312**, 1481 (2006).
[13] B. V. Mill′, E. L. Belokoneva, and T. Fukuda, Russian Journal of Inorganic Chemistry **43**, 1168 (1998).
[14] K. Marty, V. Simonet, E. Ressouche, R. Ballou, P. Lejay, and P. Bordet, Phys. Rev. Lett. **101**, 247201 (2008).
[15] V. Simonet, M. Loire, and R. Ballou, Eur. Phys. J. Special Topics **213**, 5 (2012).
[16] I. V. Yu, A. A. Mukhin, and B. V. Prokhorov, A. S. ans Mill', Solid State Phenomena **152**, 299 (2009).
[17] K. Marty, P. Bordet, V. Simonet, M. Loire, R. Ballou, C. Darie, J. Kljun, P. Bonville, O. Isnard, P. Lejay, et al., Phys. Rev. B **81**, 054416 (2010).
[18] L. Chaix, S. de Brion, F. Lévy-Bertrand, V. Simonet, R. Ballou, B. Canals, P. Lejay, J. B. Brubach, G. Creff, F. Willaert, et al., Physical Review Letters **110**, 157208 (2013).
[19] H. D. Zhou, L. L. Lumata, P. L. Kuhns, A. P. Reyes, E. S. Choi, N. S. Dalal, J. Lu, Y. J. Jo, L. Balicas, J. S. Brooks, et al., Chemistry of Materials **21**, 156 (2009).
[20] N. Lee, Y. J. Choi, and S.-W. Cheong, Applied Physics Letters **104**, 072904 (2014).
[21] The propagation vector is perpendicular to the plane of rotation of the magnetic moments for a helical order and within this plane for a cycloidal order.
[22] T. hisa Arima, Journal of the Physical Society of Japan **76**, 073702 (2007).
[23] M. Kenzelmann, G. Lawes, A. B. Harris, G. Gasparovic, C. Broholm, A. P. Ramirez, G. A. Jorge, M. Jaime, S. Park, Q. Huang, et al., Phys. Rev. Lett. **98**, 267205 (2007).
[24] A. J. Hearmon, F. Fabrizi, L. C. Chapon, R. D. Johnson, D. Prabhakaran, S. V. Streltsov, P. J. Brown, and P. G. Radaelli, Phys. Rev. Lett. **108**, 237201 (2012).
[25] J. S. White, C. Niedermayer, G. Gasparovic, C. Broholm, J. M. S. Park, A. Y. Shapiro, L. A. Demianets, and M. Kenzelmann, Phys. Rev. B **88**, 060409 (2013).
[26] K. Cao, R. D. Johnson, F. Giustino, P. G. Radaelli, G.-C. Guo, and L. He, Phys. Rev. B **90**, 024402 (2014).
[27] L. N. Bulaevskii, C. D. Batista, M. V. Mostovoy, and D. I. Khomskii, Phys. Rev. B **78**, 024402 (2008).
[28] M. Loire, V. Simonet, S. Petit, K. Marty, P. Bordet, P. Lejay, J. Ollivier, M. Enderle, P. Steffens, E. Ressouche, et al., Phys. Rev. Lett. **106**, 207201 (2011).
[29] A. Zorko, M. Pregelj, A. Potočnik, J. van Tol, A. Ozarowski, V. Simonet, P. Lejay, S. Petit, and R. Ballou, Phys. Rev. Lett. **107**, 257203 (2011),
[30] J. Jensen, Phys. Rev. B **84**, 104405 (2011).
[31] More information about the magnetic structure factor, the chirality, and neutron polarimetry can be found in the supplemental material.
[32] I. S. Lyubutin, P. G. Naumov, B. V. Mill', K. V. Frolov, and E. I. Demikhov, Phys. Rev. B **84**, 214425 (2011).
[33] V. Scagnoli, S. W. Huang, M. Garganourakis, R. A. de Souza, U. Staub, V. Simonet, P. Lejay, and R. Ballou, Physical Review B **88**, 104417 (2013).
[34] J. Jensen and A. R. Mackintosh, Rare Earth Magnetism (Clarendon Press - Oxford, 1991).
[35] C. Toulouse and et al., (submitted) (2015).
[36] C. Lee, E. Kan, H. Xiang, and M.-H. Whangbo, Chemistry of Materials **22**, 5290 (2010).